

REGULATION OF TERMINAL VOLTAGE AND OUTPUT FREQUENCY OF A VARIABLE-SPEED DUAL-EXCITED SYNCHRONOUS GENERATOR BY USING A COMPUTER-BASED TWO-PHASE EXCITATION SYSTEM

Zaipuna O. Yonah

Ahmed M. El-Serafi

Arnold E. Krause

Department of Electrical Engineering
University of Saskatchewan
Saskatoon, Saskatchewan
CANADA. S7N 0W0

Abstract: A computer-based two-phase excitation system for a variable-speed dual-excited synchronous generator (DESG) has been implemented. The excitation system has an automatic frequency regulation (AFR) scheme and an automatic voltage regulation (AVR) scheme. The two regulation schemes control the excitation currents simultaneously, but act independently, to enable the DESG to supply power at constant frequency and constant terminal voltage while its rotor is driven at a variable speed as it is in the case of wind power generation systems. This paper describes the implemented prototype of the computer-based excitation system and its performance in real time. The experimental results show that the excitation system is flexible, portable, fast acting, and accurate.

INTRODUCTION

It has been demonstrated earlier [1-2] that dual-excited synchronous generators (DESG) can be applied as non-conventional variable-speed constant-frequency (VSCF) generating systems, e.g. as wind power generating systems. In such applications, these machines, which have two excitation windings, require two-phase slip frequency excitation currents. Thus, their practical application for VSCF operation depends on the ability to generate and control these two-phase excitation currents. It has been further shown that the frequency regulation and the control of the magnitude of the generator terminal voltage can both be accomplished by controlling specific parameters of the excitation currents [3-4]. A schematic diagram of such an excitation control scheme is illustrated in Figure 1.

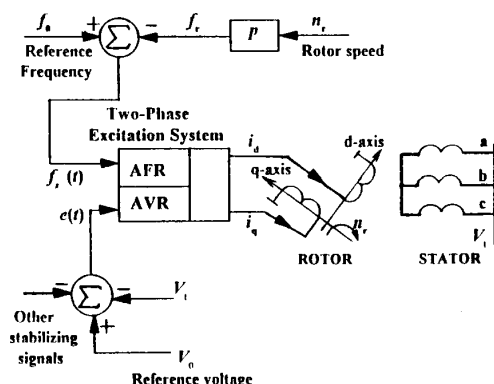


Figure 1: A two-phase excitation scheme for a variable-speed DESG.

This paper describes a two-phase computer-based excitation system for a DESG. The excitation system is implemented on a distributed computing hardware consisting of three micro-computers (PCs). The excitation system has an automatic frequency regulation (AFR) scheme and an automatic voltage regulation (AVR) scheme. Both schemes control the two-phase excitation currents simultaneously, but act independently. In addition, the paper presents test results of the real time performance of the AFR and the AVR schemes acting on a loaded laboratory DESG driven at variable speed and under different operating conditions.

EXCITATION REQUIREMENTS

To operate the DESG in a VSCF generating set up, the two field windings of the DESG should be supplied with two sinusoidal, orthogonal (i.e., 90° phase shifted from each other), variable-amplitude, variable-frequency excitation voltages. These two excitation voltage signals must have the same frequency, f_e , which must be proportional to the magnitude of the rotor slip ($s_r = |s|$ where s is the rotor slip). The phase sequence of the two excitation voltages should be controlled by the sign of the rotor slip, $\text{sign}[s]$. The amplitude of these excitation voltages, V , should be controlled by the generator terminal voltage error $e = e(t)$ in a way to nullify the deviations of the amplitude of the terminal voltage from the specified amplitude, V_0 . These excitation requirements can be fulfilled by supplying the field windings with voltages v_d and v_q described as follows:

$$v_d = V(1 - \phi(e)) \cos(2\pi s_r f_0 t) \quad (1)$$

$$v_q = V(1 - \phi(e)) \sin(2\pi s_r f_0 t) \quad (2)$$

$$s = \frac{n_s}{n_0} = \frac{n_0 - n_r}{n_0} = \frac{f_0 - f_r}{f_0} \quad (3)$$

$$f_r = p n_r \quad (4)$$

$$f_0 = p n_0 \quad (5)$$

where p is the number of pole pairs of the generator, ϕ is a control algorithm which is a function of the voltage error signal, $e(t)$, n_r is the rotor speed in rev/sec, n_0 is the synchronous speed in rev/sec, f_r is the frequency in Hz corresponding to n_r , and f_0 is the frequency in Hz corresponding to n_0 .

Assuming that the two field windings are physically identical and are electrically in quadrature to each other, the two excitation voltages will then produce two orthogonal fluxes ϕ_d and ϕ_q in the d - and q -axis windings, respectively. These two fluxes will produce a resultant flux

Φ in the airgap of the DESG. This resultant flux Φ rotates at a relative speed equal to $n_r (= s_r n_s)$ with respect to the rotor and its direction of rotation will be in the same direction as the rotor if $\text{sign}[s] = +1$, or will be in the opposite direction to that of the rotor if $\text{sign}[s] = -1$. For $\text{sign}[s] = 0$, the flux Φ will rotate together with the rotor, i.e. stationary with respect to the rotor, and this corresponds to the case of conventional d.c. current excitation. The control of the direction of rotation of Φ is possible by dynamically controlling the phase sequence of the excitation voltages v_d and v_q [3-4] and, thus, the slip sign is a sufficient control for dynamically selecting the appropriate phase sequence of the two-phase excitation voltages. With this type of excitation control, the rotation of the flux Φ can be dynamically superimposed on the mechanical rotation, n_r , to realize a constant armature frequency. On the other hand, the magnitude of the resultant flux Φ should be such that the terminal voltage is kept constant.

EXCITATION SYSTEM PROTOTYPE

Figure 2 shows the block diagram of the prototype of the computer-based two-phase excitation system. In this figure, PC1, PC2, and PC3 are three AT & T 8086/10 MHz micro-computers with bus speeds of 5 MHz. Each PC has a computer-interfaced two-channel, 12-bit, bipolar and inverting, multiplying digital-to-analog converter. The channels are identified as DAC_{x1} and DAC_{x2}, where x is the PC number, i.e. $x = 1, 2$, or 3 . The PCs have a set of electronic programmable real-time timers (built around the 8254 timer chip). These timers are used for frequency synthesis and frequency or pulse-width measurements. In addition, each PC has an 8-channel analog-to-digital converter (ADC) (DAS-8 cards) for data acquisition. In Fig. 2, only the ADC in PC1 is shown. The microcomputer PC1 uses the ADC to measure the output terminal voltage of the generator via an RMS-to-DC converter circuit (AD536). The amplifiers BOPA1 and BOPA2 (KEPCO-BOP 15 V-20 A (M)) are used to amplify the control signals v_d and v_q . The dual-excited synchronous generator is identified as DESG in Fig. 2. A shaft encoder capable of producing 360 ppr is used to monitor the speed of the rotor at a resolution of 0.01667 rpm. The generator is driven by a dc motor which is labelled as the prime mover in Fig. 2. This figure also shows a bidirectional, programmable, 24-bit parallel data line connecting PC2 and PC3. This data line is configured using two PIO-12 plug-in-cards, one on each PC. The microcomputer PC2 receives coded data containing module status, phase-sequence and the value of number of samples per cycle, N , from PC3 via this data line. The value of N is used in PC2 to select a pattern of data corresponding to one cycle of a sinusoidal wave. The selected pattern is used for signal generation using DAC₂₁ and DAC₂₂. The sample rate of application of the pattern data to these two DACs is controlled by a frequency modulated (FM) square wave signal from PC3 which is fed through a digital I/O port in PC2. The FM signal has a frequency Nf_s and is generated using programmable counters in PC3. Another square wave signal which has a frequency of $f_{REF}/2$ (generated in PC1) is used to synchronize the sampling operations in PC1 and PC3. The methodology for generating the two-phase excitation voltages using a computer-based technique has been reported previously in References [3].

It should be noted that Equations (1) and (2) have two factors, i.e. $V(1 - \phi(e))$ and $\cos(2\pi s_a f_0 t)$ or $\sin(2\pi s_a f_0 t)$, which should be multiplied in real time on a continuous basis to adjust the amplitude of the excitation voltages v_d and v_q . This multiplication can be accomplished by software or hardware multiplication. Of these two types of multiplications, the software multiplication is slower and, thus, hardware multiplication is preferred. Hardware multiplication can be accomplished by using co-processors or multiplying DACs. However, the sampling processes in PC1 and PC3 are mainly data acquisition

processes which are driven at a selectable constant sample rate. On the other hand, the sampling process in PC2 is driven at a variable sample rate which is controlled by the variable-frequency FM signal from PC3. Thus, the multiplication of the two factors in Eqns (1) and (2) cannot be done in one PC and, thus, only the use of multiplying DACs is feasible. In Fig. 2, the hardware multiplication is implemented by having the reference supply, U_{REF} , of DAC₂₁ and DAC₂₂ (in PC2) controlled by the output of DAC₁₂ in PC1. In this case, the waveform of U_{REF} is programmable in software. Details of the on-line programming of U_{REF} using the multiplying DACs is reported in reference [4].

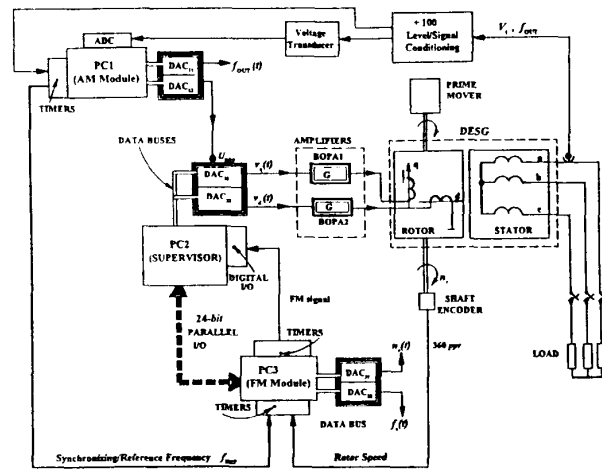


Figure 2: A block diagram of the two-phase computer-based excitation system supplying a DESG.

RESULTS AND DISCUSSION

The prototype excitation system is being tested on a 3-phase, 3000 VA, 208 V, 60 Hz, 1800 rpm, Star-connected DESG. The results present the response of the loaded DESG to the variation of the rotor speed for four cases, namely, when both the AFR and AVR schemes are OFF, when the AFR scheme is ON and the AVR scheme is OFF, when the AFR scheme is OFF and the AVR scheme is ON, and when both the AFR and AVR schemes are ON. The amplifiers BOPA1 and BOPA2 (Fig. 2) are rated for 300 VA each and were set to have the same gain $G = 9$. Seven signals were recorded simultaneously to monitor the generator response. These are V_t , f_{OUT} , f_s , n_r , v_d , v_q , and U_{REF} as shown in Fig. 2. In the presented results, a positive sign (+) prefix denotes slip frequencies that correspond to speeds below the synchronous speed and, a negative sign (-) prefix denotes slip frequencies that correspond to speeds above the synchronous speed. The chart sensitivities for all plots are as follows: horizontal- 0.5 sec./div. for all plots, vertical- plots (a), (b) and (c) 200 mV/div., plot (d) 18 rpm/div., plots (e) and (f) 0.6 Hz/div., and plot (g) 10 V/div..

(A.) Response to Speed Variation When the AFR and the AVR Schemes are Both OFF

Figure 3 shows the response of the DESG to variation in the rotor speed when there is no frequency and voltage control, i.e. the AFR and the AVR schemes are both OFF. In this figure, $U_{REF} = -4.6$ V, the reference frequency $f_{REF} = 60.2$ Hz, and the frequency of the excitation voltages, v_d and v_q was set at 3.3 Hz. The phase sequence was selected such that the direction of field rotation was the same as that of the rotor. The speed was varied from ~ 1368 rpm to ~ 1908 rpm. The output frequency varied from ~ 48.9 Hz to ~ 66.9 Hz. This output frequency

can be described by $f_{OUT} = f_r + 3.3 \text{ Hz}$. The magnitude of the output terminal voltage varied from $\sim 155 \text{ V}$ to $\sim 200 \text{ V}$. These results show that without the frequency and voltage regulation, the DESG driven at variable speed will generate voltage with variable amplitude and variable frequency.

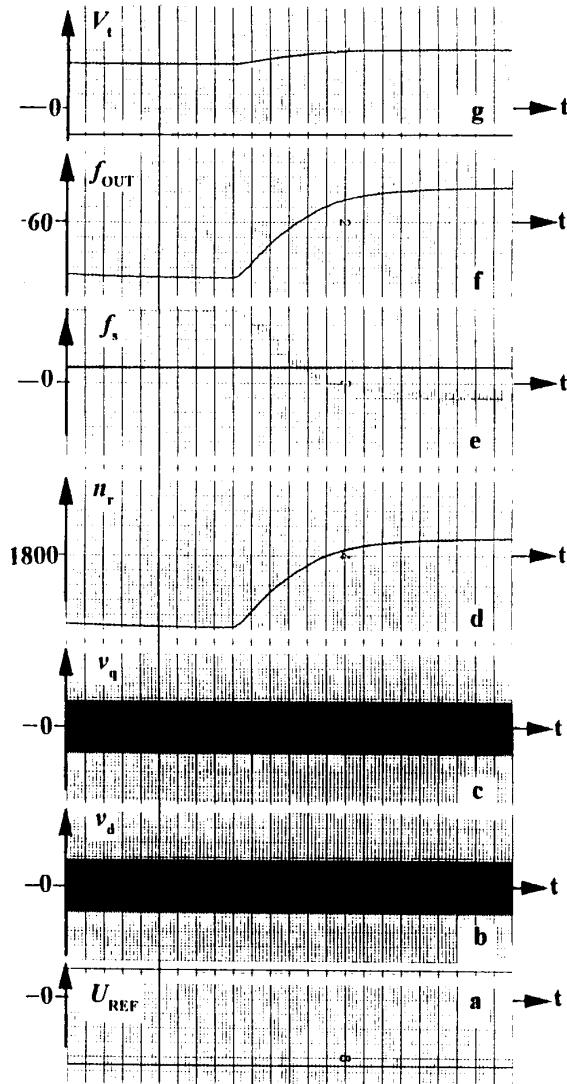


Figure 3: Real-time response of the DESG to speed variation when the AFR and the AVR schemes are both OFF.

(B.) Response to Speed Variation When the AFR Scheme is ON and the AVR Scheme is OFF.

The results for this test are shown in Figure 4. In this figure, $f_{REF} = 60.2 \text{ Hz}$, $U_{REF} = -4.6 \text{ V}$. The speed was varied from $\sim 1665 \text{ rpm}$ to $\sim 1944 \text{ rpm}$. Correspondingly, the slip frequency varied from $\sim +4.5 \text{ Hz}$ to $\sim 4.8 \text{ Hz}$ (i.e. a slip variation of $\sim +7.47\%$ to $\sim -7.97\%$). The output frequency was $\sim 60.2 \text{ Hz}$ with an error of less than 0.1% . The frequency control in this case can be described by $f_{OUT} = f_r + \text{sign}[s] \cdot f_s$. The output voltage overshoot from $\sim 140 \text{ V}$ to $\sim 380 \text{ V}$ near the dc excitation (zero slip) and then settled back to 140 V . This is due to the fact that the load was not changed. Further, Figures 4(b) and (c) show the effectiveness of the AFR scheme in controlling the phase sequence of the two excitation voltages as the speed varies from subsynchronous to supersynchronous speeds.

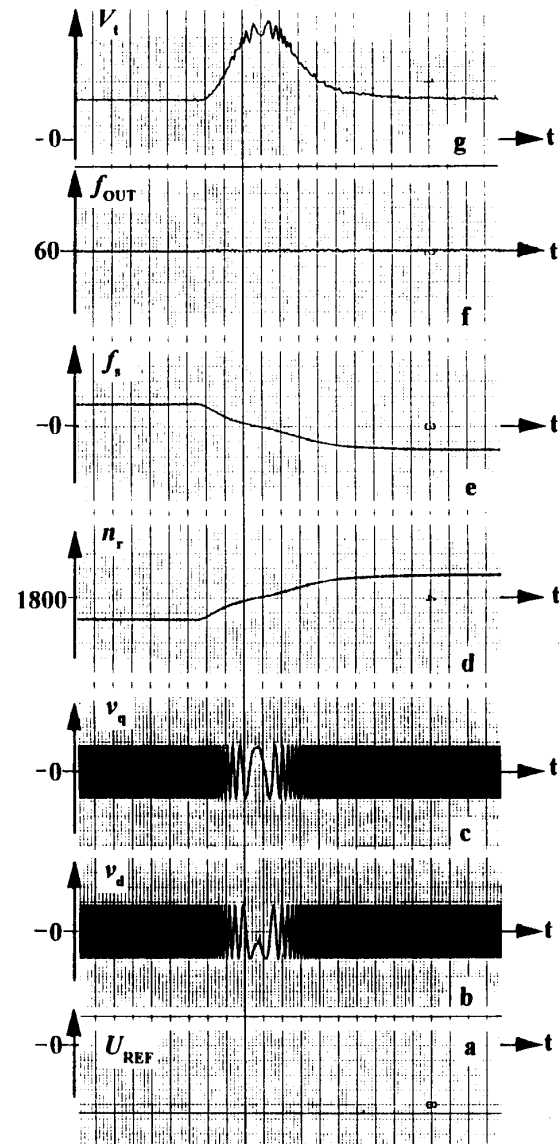


Figure 4: Real-time response of the DESG to speed variation when the AFR scheme is ON and the AVR scheme is OFF.

(C.) Response to Speed Variation When the AFR Scheme is OFF and the AVR Scheme is ON.

The excitation frequency in this case was set at $\sim +4.5 \text{ Hz}$ and $f_{REF} = 60.2 \text{ Hz}$. The reference output voltage was set at 195 V . The speed was varied from $\sim 1674 \text{ rpm}$ to $\sim 1944 \text{ rpm}$. This resulted in U_{REF} varying from $\sim -6.1 \text{ V}$ to $\sim -5.4 \text{ V}$ to regulate the output voltage and the error in the output voltage was less than 1% . Since the AFR scheme was OFF, the output frequency varied with the speed from $\sim 60.2 \text{ Hz}$ to $\sim 69.3 \text{ Hz}$ as shown in Fig. 5(f). In this test, $f_{OUT} = f_r + 4.5 \text{ Hz}$.

(D.) Response to Speed Variation When the AFR and the AVR Schemes are Both ON.

Figure 6 illustrates the performance of the complete excitation system for the case when $f_{REF} = 60.2 \text{ Hz}$ and the desired output voltage set to 195 V . In this figure, the speed was varied from $\sim 1701 \text{ rpm}$ to $\sim 1935 \text{ rpm}$. Consequently, the slip frequency varied from $\sim +3.3 \text{ Hz}$

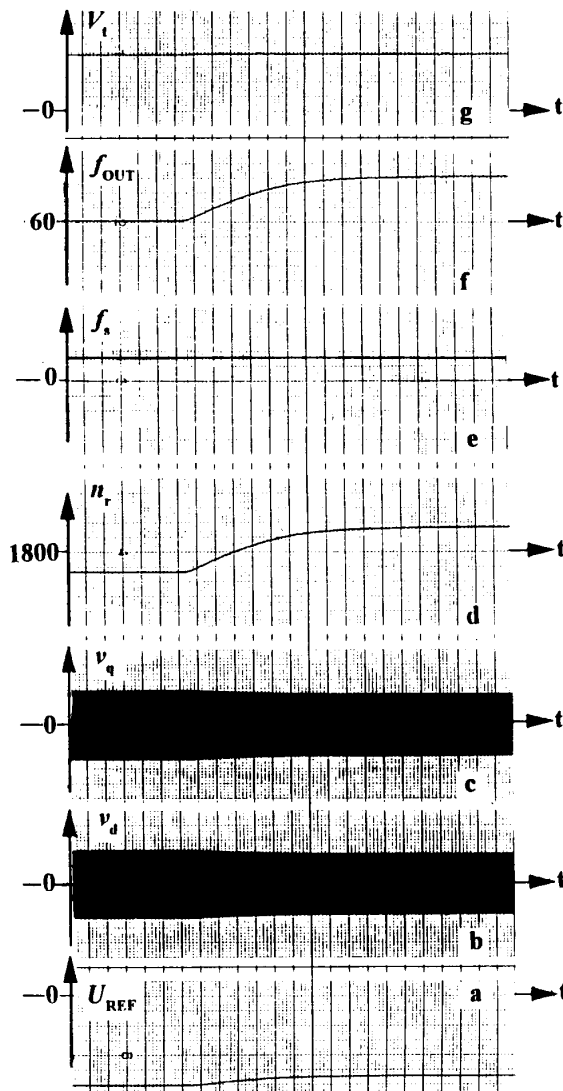


Figure 5: Real-time response of the DESG to speed variation when the AFR scheme is OFF and the AVR scheme is ON.

to ~ 4.5 Hz. Figures 6(f) and (g) clearly shows the effectiveness of the AFR and the AVR schemes. Qualitatively, it can be summarized that, with the AFR and the AVR schemes both ON, the frequency, the amplitude, the frequency range, the phase sequence of the excitation voltages and the parameters of the controllers for both regulation schemes, can all be controlled dynamically in real time.

CONCLUSIONS

This paper has described a prototype of a computer-based two-phase excitation system for a variable-speed dual-excited synchronous generator. Also, some results showing the real-time performance of the excitation system have been presented. The results show that the excitation system is flexible, portable, fast acting, and accurate. The superiority of the excitation system, which is based on intelligent signal instrumentation, is in that the frequency, the amplitude, the waveform distortion, the frequency-range, the phase sequence of the two-phase excitation currents, and the parameters of the controllers for both the AFR and the AVR schemes, can all be controlled dynamically in real time for performance optimization.

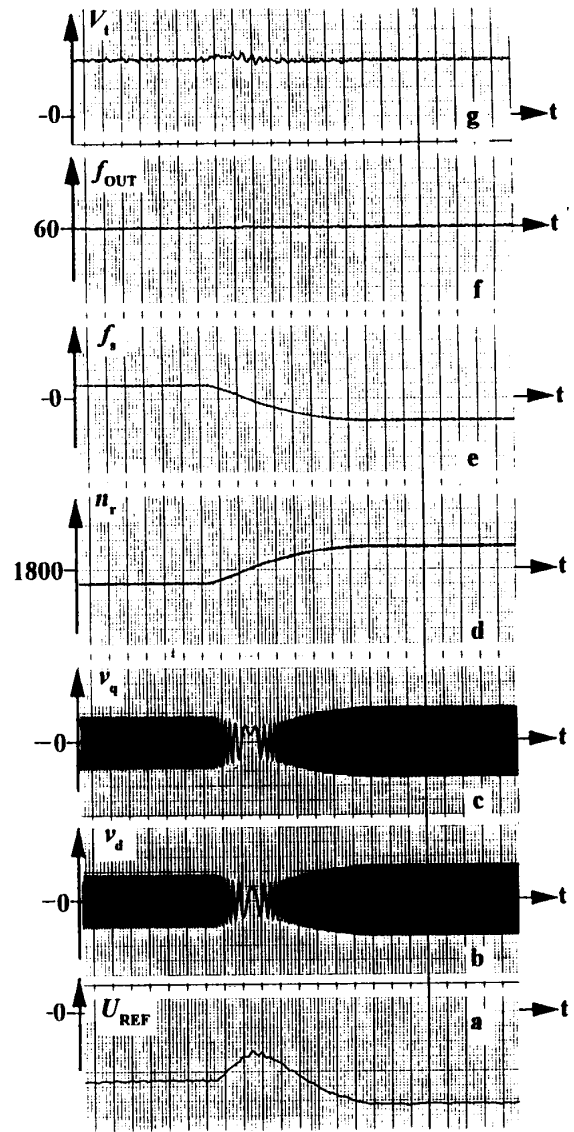


Figure 6: Real-time response of the DESG to speed variation when the AFR and the AVR schemes are both ON.

REFERENCES

- [1] M. S. Morsy, H. H. Amcr, M. A. Badr and A. M. El-Serafi, "Transient Stability of Synchronous Generators with Two-Axis Slip Frequency Excitation", *IEEE Transactions on Power Apparatus and Systems*, Vol. PAS - 102, 1983, pp. 852-1004.
- [2] S. Hayashi, et al., "Development of Adjustable Speed Generator", *International Conference on Large High Voltage Electric Systems (CIGRE)*, Paper No. 11-03, Paris, 1988.
- [3] Z. O. Yonah, A. M. El-Serafi and A. E. Krause, "Computer-Based Real-Time Excitation Control Algorithm for a Variable-Speed Dual-Excited Synchronous Generator", *Proceedings of the Canadian Conference on Electrical and Computer Engineering*, Quebec, Canada, September 25-27, 1991, pp. 64.1.1 - 64.1.4.
- [4] Z. O. Yonah, A. M. El-Serafi and A. E. Krause, "Performance of a Computer-Based Two-Phase Excitation system for a Variable-Speed Dual-Excited Synchronous Generator", *Proceedings of the WESCANEX Conference on Communications, Computers and Power in the Modern Environment*, Saskatoon, Canada, May 17 - 18, 1993, pp. 263 - 268.